Immunity, Vol. 15, 847–859, November, 2001, Copyright ©2001 by Cell Press

Role of Calcium Influx in Cytotoxic T Lymphocyte Lytic Granule Exocytosis during Target Cell Killing

Taras A. Lyubchenko, Georjeana A. Wurth, and Adam Zweifach[1]
Department of Physiology and Biophysics and Department of Immunology
University of Colorado Health Sciences Center
4200 East 9th Avenue
Denver, Colorado 80262

Summary

One mechanism cytotoxic T lymphocytes use to kill targets is exocytosis of cytotoxic agents from lytic granules, a process that requires Ca^{2+} influx. We investigated the role of Ca^{2+} influx in granule exocytosis using TALL-104 human leukemic cytotoxic T cells triggered via a bispecific antibody containing an anti-CD3 F(ab′) to kill Raji B lymphoma cells. Using a novel fluorescence method, we detected target-directed release of ~15% of lytic granules during killing. Consistent with previous work, we observed sustained CTL Ca^{2+} gradients during killing, but gradients reflect the behavior of Fura-2 in granules. Rapid imaging experiments suggest that Ca^{2+} channels are not polarized during killing, indicating that Ca^{2+} influx does not direct granule reorientation. Furthermore, we find that Ca^{2+} acts via a high-affinity interaction to promote granule exocytosis.

Introduction

Cytotoxic T lymphocytes (CTLs) kill virus-infected, tumor, and non-self targets (Berke, 1994; Griffiths, 1995). One important mechanism used is exocytosis of cytotoxic agents, such as perforin and granzymes, from preformed lytic granules that are secretory lysosomes (Griffiths and Argon, 1995; Stinchcombe and Griffiths, 1999). These dual-function organelles contain lysosomal proteins, are acidic, take up lysosomotrophic probes, and are connected to the endocytic pathway (Burkhardt et al., 1990; Griffiths and Argon, 1995).

Granule exocytosis-mediated target cell killing and T cell receptor (TCR) stimulated granule exocytosis require extracellular Ca^{2+} (Ca^{2+}_o) (Takayama and Sitkovsky, 1987), suggesting that step(s) in the process require increases in intracellular [Ca^{2+}] ([Ca^{2+}]$_i$). Consistent with this idea, stimulation of cells with ionomycin and phorbol esters can substitute for stimulation via TCR/ CD3 in promoting granule exocytosis, but neither agent is effective alone (Berebi et al., 1987; Lancki et al., 1987). However, the role of [Ca^{2+}]$_i$ increases in lytic granule exocytosis is unclear, and the affinity of the Ca^{2+}-dependent step(s) involved has not been determined. Exocytosis in different secretory cell types displays a wide range of affinities for Ca^{2+}, and a correspondingly wide range of delays between increases in [Ca^{2+}] and exocytosis. In some fast synaptic terminals, the interaction is low affinity (K_d 10–150 μM), and the delay between influx exocytosis is short (1 ms or less) (Zucker, 1996). At the other extreme, in mast cells, the interaction is high affinity (K_d < 1 μM), and the delay between influx and exocytosis is long (10 s or more) (Hide et al., 1993; Kim et al., 1997). These functional differences are thought to reflect the participation of Ca^{2+}-sensitive molecules with different affinity, and whether or not Ca^{2+} acts in near membrane microdomains, where [Ca^{2+}] can be substantially higher than in the bulk cytosol. Determining the affinity of the Ca^{2+}-dependent step(s) in CTL lytic granule exocytosis is an important prerequisite for identifying Ca^{2+}-dependent molecule(s) that may participate in release.

A unique feature of CTL granule exocytosis is that granules are released specifically at the point of contact with the target (Yanelli et al., 1986; Kupfer and Singer, 1989). This target-directed exocytosis ensures that only the cell to which the CTL is bound is lysed. If contact between CTL and target occurs with granules located away from the contact site, then granules reorient before release. One possible action of [Ca^{2+}]$_i$ increases in granule exoyctosis has been suggested by studies that showed that reorientation of the killer cell's microtubule-organizing center (MTOC) and Golgi to face the target cell, requires Ca^{2+}_o (Kupfer and Singer, 1989). This suggests that [Ca^{2+}]$_i$ plays a role in movement of lytic granules to the site of contact with the target. Intriguingly, Poenie et al. reported sustained [Ca^{2+}]$_i$ gradients, due to influx in CTLs in contact with relevant targets; [Ca^{2+}]$_i$ was persistently elevated at the rear of the CTL, away from the site of contact with the target (Poenie et al., 1987), leading to the proposal that [Ca^{2+}]$_i$ gradients generated by influx may direct the reorientation of lytic granules (Poenie et al., 1987; Griffiths and Argon, 1995). However, the results described above are contradicted by another study that also reported sustained [Ca^{2+}]$_i$ gradients (Gray et al., 1988), but found that the region of higher [Ca^{2+}]$_i$ was localized at the site of contact with the target, and apparently reflects the fact that the lytic granules, which were localized at the rear of the cell in these experiments, did not participate fully in the [Ca^{2+}]$_i$ rise. Thus, the issue of the existence of sustained [Ca^{2+}]$_i$ gradients due to polarized influx and their possible role in granule exocytosis, remains unclear.

We examined the role of [Ca^{2+}]$_i$ increases in bispecific antibody (bsAb)-stimulated granule exocytosis-mediated target cell killing by TALL-104 human leukemic CTLs (Cesano and Santoli, 1992). Our results indicate that target-directed granule exocytosis can occur without polarized Ca^{2+} influx, suggesting that Ca^{2+} influx does not play a role in directing granule reorientation, and that Ca^{2+} has an action at a large diffusional distance from channels, which indicates that one way Ca^{2+} promotes granule exocytosis is via a high affinity interaction. However, we cannot exclude the possibility that there are multiple Ca^{2+}-dependent steps involved.

[1] Correspondence: adam.zweifach@uchsc.edu

Results

A Bispecific Antibody Triggers TALL-104 to Kill Raji B Cells

Tall-104 cells kill a variety of tumor cells in a non-MHC restricted fashion (Cesano and Santoli, 1992), but the molecule(s) involved in tumor-cell recognition are unknown. We used a bispecific antibody (bsAB) consisting of an F(ab′) targeted against an HLA-DR epitope expressed on malignant B cells, coupled by a FOS/JUN interaction to an anti-CD3 F(ab′) (Link et al., 1998), to trigger TCR-dependent killing of Raji B lymphoma cells by TALL-104. BsAB-treated Raji cells stimulated $[Ca^{2+}]_i$ increases in TALL-104 cells (Figures 1A and 1C), while untreated Raji cells did not (Figure 1C). In these experiments, Fura-2 loaded TALL-104 cells were adhered to coverslips, and bsAB-treated Raji cells were dropped onto them. $[Ca^{2+}]_i$ signals elicited by target cell contact were heterogeneous, often consisting of repetitive oscillations from baseline levels of 50–100 nM to values ranging from 300 to 2000 nM. When TALL-104 cells were stimulated with bsAB-treated Raji cells in the absence of $Ca^{2+}{}_o$, responses were smaller and more transient (Figures 1B and 1C), indicating that influx contributes to $[Ca^{2+}]_i$ elevations observed in the presence of $Ca^{2+}{}_o$.

BsAB-treated Raji cells elicit TALL-104 granule exocytosis, but untreated Raji cells do not (Figure 2). In these experiments, Raji cells loaded with calcein were adhered to coverslips. An excess of TALL-104 cells was added to the chamber, and allowed to settle into contact with the Raji cells. Approximately 140 s after TALL-104 addition, bsAB-treated Raji cells began to exhibit sudden decreases in calcein fluorescence (Figure 2B), consistent with dye leakage through perforin pores inserted via granule exocytosis (Lichtenfels et al., 1994; Zweifach, 2000). To analyze the time-course of target cell killing, we computed a cumulative latency distribution for killing from traces like those shown in Figure 2B for all of the cells in the experiment (Figure 2C). Within ~1000 s, 70% of Raji cells had been killed.

Further evidence that calcein fluorescence decreases reflect perforin pore formation comes from experiments performed in Ca^{2+}-free Ringer's. Fluorescence decreases were not observed until after $Ca^{2+}{}_o$ was added (Figure 2C, bottom), consistent with the Ca^{2+}-dependence of granule release and/or the Ca^{2+}-dependence of perforin pore formation. Under these conditions, killing began 40–60 s after $Ca^{2+}{}_o$ addition. We find that formation of perforin pores requires 40–60 s (see below), and this result suggests that some CTLs may undergo exocytosis immediately upon initiation of Ca^{2+} influx. However, the slow time course of the bulk of killing indicates that in the majority of CTLs exocytosis occurs with a substantial delay after $[Ca^{2+}]_i$ is elevated. Although the delay until killing began was shorter when cells interacted first in the absence of $Ca^{2+}{}_o$, the maximum rate at which target cells were killed following Ca^{2+} addition was not appreciably faster than the rate at which targets were killed when contact was made in the presence of $Ca^{2+}{}_o$ (compare Figure 2B top and bottom). In three experiments conducted in the presence of $Ca^{2+}{}_o$, the maximal rate of killing observed was $0.54 \pm 0.12\%\ s^{-1}$, and occurred 350 ± 37.9 s after addition of TALL-104 cells. In three experiments in which contacts were made in the absence of $Ca^{2+}{}_o$, the maximal rate of killing was $0.56 \pm 0.16\%\ s^{-1}$, and occurred 100 ± 40 s after $Ca^{2+}{}_o$ addition. The difference in delay reflects the time needed for cells to form conjugates and initiate signaling in experiments conducted in the presence of $Ca^{2+}{}_o$ (200–300 s, Figure 1).

Consistent with the results of calcein experiments, bsAB-treated Raji cells stimulated release of granzyme A as detected by BLT-esterase assays, but untreated Raji cells did not (Figure 2D). Granzyme release required the presence of $Ca^{2+}{}_o$ (Figure 2D), confirming that Ca^{2+} influx is required for bsAB-stimulated exocytosis of lytic granules from TALL-104. That exocytosis, as detected by BLT-esterase assays, requires $Ca^{2+}{}_o$ suggests that the $Ca^{2+}{}_o$-dependence of target cell killing seen in Figure 2C, reflects the $[Ca^{2+}]_i$-dependence of granule exocytosis rather than the $Ca^{2+}{}_o$-dependence of perforin pore formation.

BsAB-Stimulated Exocytosis Is Target Directed

To determine whether bsAB-stimulated target cell killing by TALL-104 involves target-directed exocytosis of lytic granules, we developed a fluorescence method for visualizing lytic granule dynamics in living cells. CTL lytic granules are secretory lysosomes (Griffiths and Argon, 1995; Stinchcombe and Griffiths, 1999), and should be labeled by fluorescent lysosmotrophic probes like lysotracker red (LTR). Lysotracker dyes have been used to monitor exocytosis of lamellar bodies from type II alveolar cells (Haller et al., 1998). Figure 3A shows an image of a living TALL-104 cell in the presence of 100 nM LTR and 3.2 μM FM1-43, a fluorescent lipophilic probe (Betz et al., 1996) used to label the plasma membrane. This rather elongated cell was crawling up and to the left. LTR labeled structures whose size (~0.5–1 μm) and location at the cell's trailing end are consistent with the idea that they are lytic granules (Griffiths and Argon, 1995). To confirm this, we incubated cells with LTR, fixed and then permeabilized them, and stained them with a FITC-conjugated antiperforin monoclonal antibody. Figure 3B is a montage of three cells processed in this manner. There is good overlap between lysotracker and perforin staining, suggesting that LTR can be used to monitor lytic granules in living cells.

To assess lytic granule dynamics (Figure 4), we loaded bsAB-treated Raji cells with calcein and adhered them to coverslips. Fura-2-loaded TALL-104 cells were preincubated with 100 nM LTR for 5 min in Ringer's solution, and then added to the experimental chamber in the presence of Ringer's solution that contained LTR. We used a 100× objective, with an adjustable numerical aperture set to 0.7, to maximize the focal depth of the images and minimize the effects of granule movements in the z-axis. In the experiment shown in Figure 4, the TALL-104 made contact with its granules initially distributed on the bottom half of the cell. Following contact, $[Ca^{2+}]_i$ increased in the TALL-104, which changed shape as it bound to the target, assuming a characteristic conjugate morphology (Yanelli et al., 1986; Poenie et al., 1987; Gray et al., 1988). As the TALL-104 changed shape, the granules simultaneously became concentrated in a denser mass located near the site of contact with the target (note that the example in Figure 4 shows

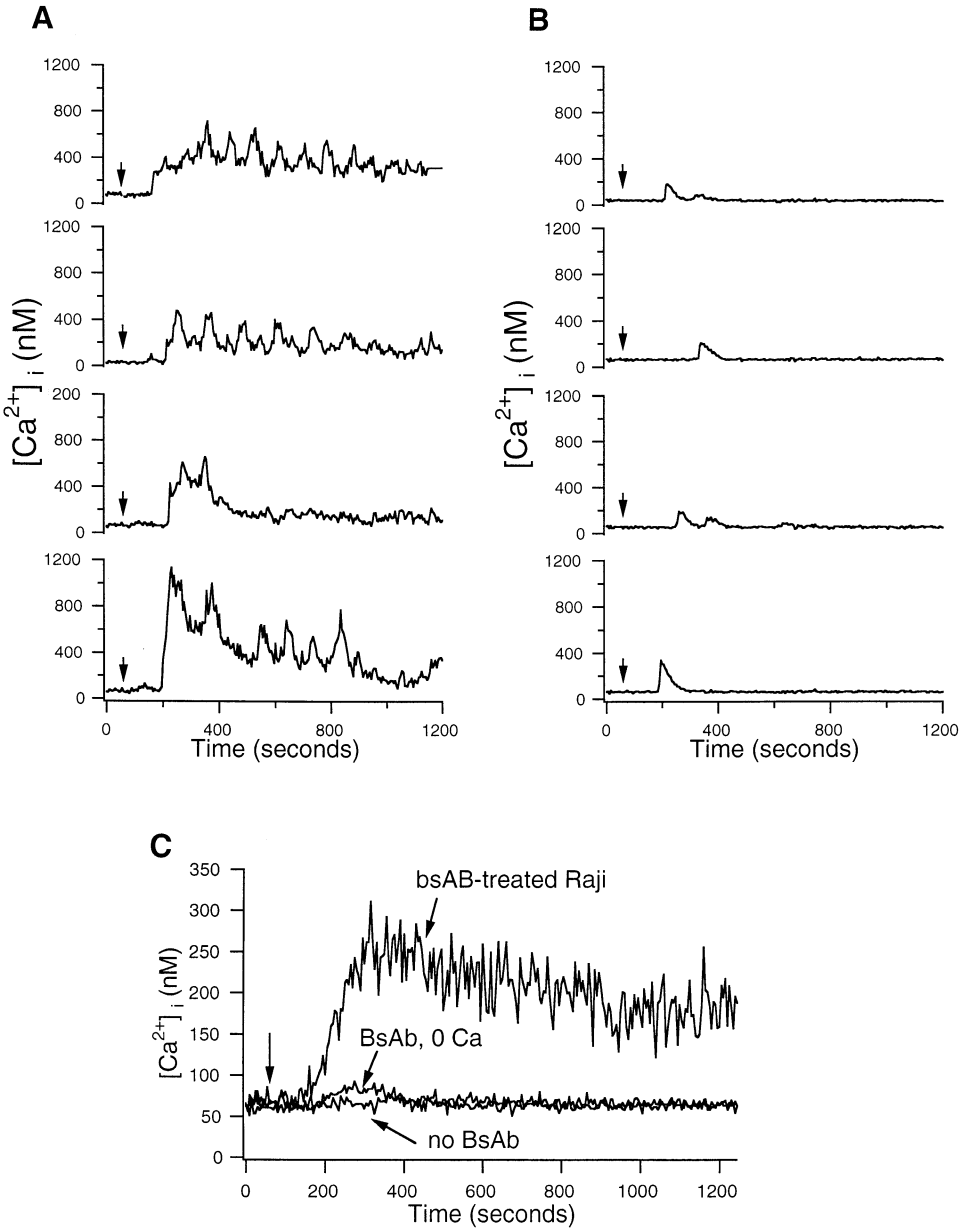

Figure 1. Contact with Bispecific Antibody-Treated Raji Cells Triggers TALL-104 $[Ca^{2+}]_i$ Increases

(A) $[Ca^{2+}]_i$ measured in single Fura-2 loaded TALL-104 cells in the presence of 2 mM $Ca^{2+}{}_o$.

(B) $[Ca^{2+}]_i$ measured in single Fura-2 loaded TALL-104 cells in the absence of $Ca^{2+}{}_o$.

(C) Average $[Ca^{2+}]_i$ in TALL-104 cells exposed to bsAB-treated Raji cells in the presence or absence of $Ca^{2+}{}_o$, or to untreated Raji cells. Traces are the average of 115 cells with bsAB, $Ca^{2+}{}_o$ = 2 mM, 88 cells without $Ca^{2+}{}_o$ and 100 cells without bsAB, respectively. Arrows indicate time of addition of bsAB-treated Raji cells.

a rather modest granule movement; more pronounced examples demonstrating reorientation were observed, see Figure 5). Finally, granules disappeared from the region of the TALL-104 in contact with the Raji cell coincident with the decrease in Raji cell calcein fluorescence. The second increase in $[Ca^{2+}]_i$ was part of a pattern of oscillations as in Figure 1A.

Initial increases in CTL $[Ca^{2+}]_i$ preceded target cell killing by 251 ± 37 s (n = 22). When similar experiments were performed in the absence of LTR, the average delay between the $[Ca^{2+}]_i$ increase and target cell killing was 218 ± 27 s (n = 35), demonstrating that LTR does not affect the kinetics of target cell killing. Quantitative analysis of changes in LTR fluorescence was complicated by the fact that Raji cells also contain structures that label with LTR, and TALL-104 cells change shape markedly during their interaction with Raji cells. Static regions of interest (ROIs) could not be used, so we selected them dynamically (see Experimental Procedures). In the example shown in Figure 4, LTR fluorescence decreased by 34.7%, coincident with loss of calcein fluorescence from the Raji cell. We were able to detect

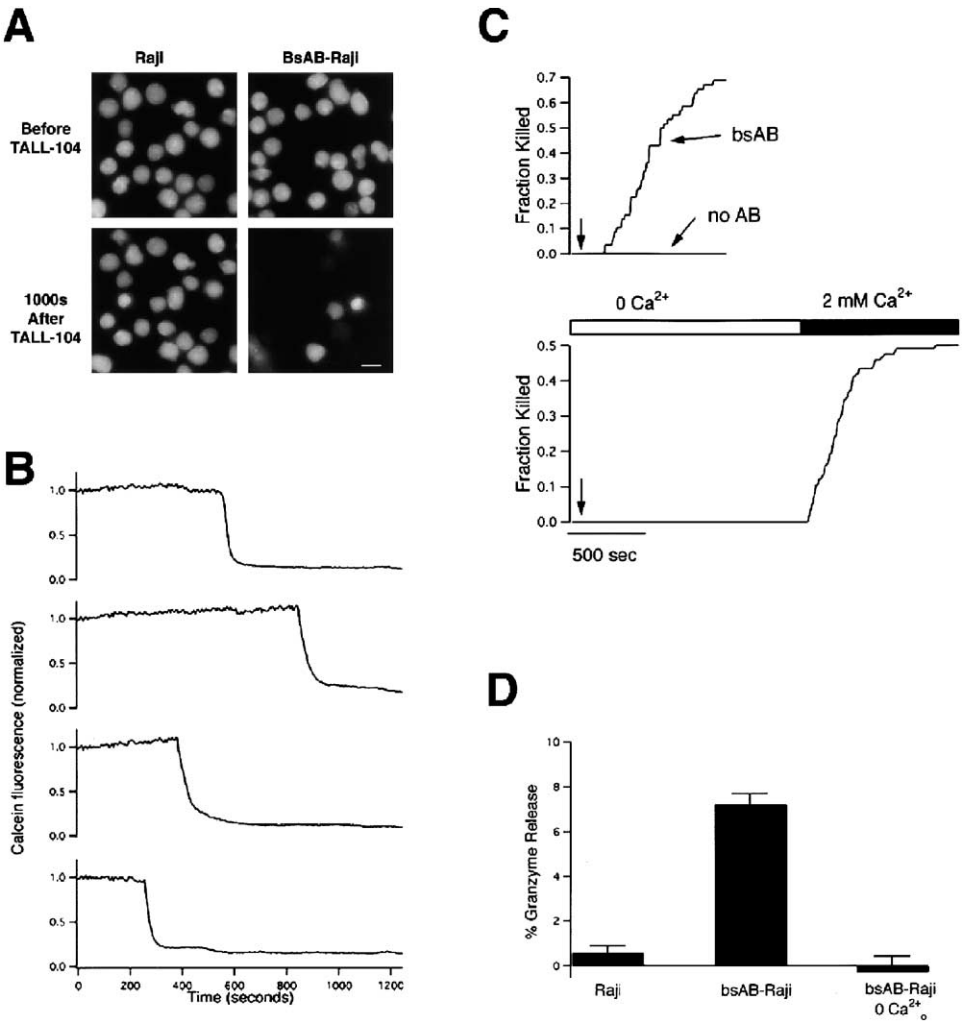

Figure 2. Bispecific Antibody-Treated Raji Cells Are Killed by TALL-104 via Lytic Granule Exocytosis

(A) Calcein-loaded Raji cells before and 1000 s after addition of an excess of TALL-104. Scale bar is 10 μm.

(B) Calcein fluorescence traces from four cells shown in (A).

(C) Top: time course of killing (loss of membrane integrity) of control and bsAB-treated Raji cells computed from traces like those shown in (B). Traces represent the time course of killing of 54 cells (+bsAB) and 60 cells (no AB) from a single representative experiment. Bottom: killing of bsAB-treated Raji cells requires Ca^{2+}_o. An excess of TALL-104 was allowed to settle onto bsAB-treated Raji cells in the absence of Ca^{2+}_o. After ~1500 s, the chamber was perfused with Ringer's. Trace compiled from the time course of killing of 124 cells from a single representative experiment.

(D) BLT-esterase assays confirm that bsAB-treated Raji cells stimulate granule exocytosis but that untreated Raji cells do not, and that Ca^{2+}_o is required for exocytosis. Data are averages of three experiments.

decreases in LTR fluorescence in thirteen of twenty-two TALL-104/ Raji interactions. In the remaining cases, granules could be seen by eye to disappear at the site of contact with the target, but corresponding decreases in LTR fluorescence could not be measured. Decreases in LTR fluorescence of 15.7 ± 2.4% occurred 63 ± 12 s before the beginning of the decrease in target cell calcein fluorescence.

When the initial contact occurred, such that LTR-labeled structures were away from the site of contact, LTR fluorescence moved toward the target before killing was detected as a sudden drop in calcein fluorescence. Most commonly, LTR-labeled structures moved as a mass in a circular motion around the cell's perimeter, although in one case it appeared that only a single structure moved. Reorientation was a slow process that typically required several hundred seconds (Figure 5A). Interestingly, cells that made contact with their granules oriented toward targets did not kill targets faster than cells that made contact with their granules in other orientations. The delay between CTL $[Ca^{2+}]_i$ increases and drops in target cell calcein fluorescence was 243 ± 55 s for cells in which granules were oriented toward the target (n = 12), 261 ± 73 s for cells in which the granules were oriented away from the target (n = 5), and 264 ± 88 s for cells in which the granules were in an intermediate orientation (n = 5). These results suggest that reorientation of lytic granules is not a rate limiting step in granule exocytosis.

Decreases in LTR fluorescence that were observed

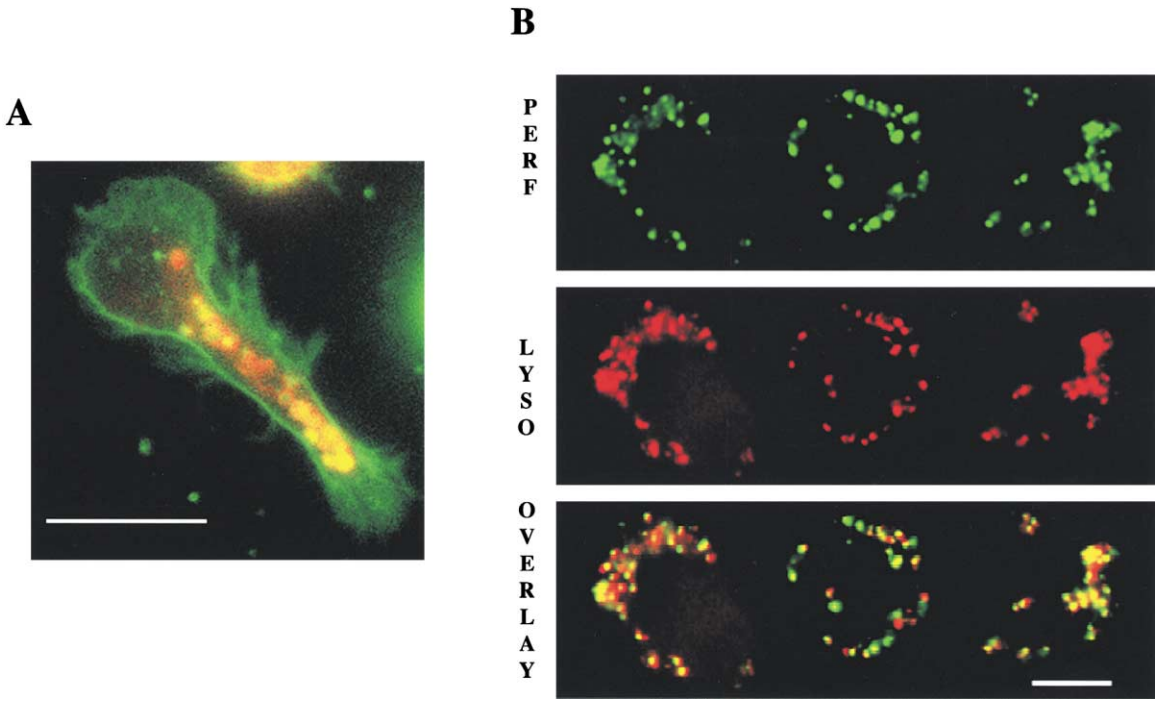

Figure 3. Lysotracker Red Labels Lytic Granules

(A) Lysotracker red staining in a living CTL. 3.2 μM FM-143 was used to stain the plasma membrane (this cell was crawling up and to the left). Scale bar is 10 μm.

(B) Comparison of the pattern of lysotracker red staining with immunolocalization of perforin (montage of three cells). Scale bar is 5 μm.

prior to target cell killing provides support for the idea that LTR labels lytic granules, and further, constitutes direct experimental confirmation of the granule exocytosis model of target cell killing. That granules disappeared at the point of contact with target cells indicates that bsAB stimulates target-directed lytic granule exocytosis. When similar experiments were conducted in Ca^{2+}-free Ringer's solution, TALL-104 cells adhered to bsAB-treated Raji cells and dynamically changed shape suggesting that Ca^{2+} influx is not required for these stages of the lytic interaction between TALL-104 and bsAB-treated Raji cells. Consistent with the results shown in Figure 2B, target cell killing and decreases in LTR fluorescence were not observed in Ca^{2+}-free Ringer's solution, but were observed after $Ca^{2+}{}_o$ was added (Figure 4C). When similar experiments were performed in Ringer's with Raji cells that had not been pretreated with bsAB, contacts between TALL-104 and Raji cells were transient, and only in rare cases appeared to lead to the formation of conjugates, confirming that the bsAB is critical for mediating the interaction between the cells.

Despite Apparent $[Ca^{2+}]_i$ Gradients, Ca^{2+} Channels Are Not Polarized during Target Cell Killing

Fura-2 ratio images from experiments like the one shown in Figure 4 revealed $[Ca^{2+}]_i$ gradients (Figure 5A, left). Regions of lower $[Ca^{2+}]_i$ corresponded to the position of the lytic granules as determined by LTR staining (Figure 5A, right). Images acquired with higher spatial resolution (including z-axis resolution) also revealed gradients (Figure 5B), but inspection of F380 images indicates that Fura-2 fluorescence corresponding to lytic granules was only sometimes brighter than non-granule fluorescence, and there was no apparent compartmentalization of dye in nuclei (staining cells with acridine orange revealed fairly abundant cytoplasm (not shown)). Lytic granules contain Ca^{2+}-buffer proteins such as calreticulin (Griffiths and Argon, 1995), and might be able to regulate their $[Ca^{2+}]$ separately from the cytosol. Alternatively, Fura-2 in granules might behave differently than cytosolic Fura-2, as the microenvironment in granules is different than in cytosol and Fura-2 is sensitive to its environment (Roe et al., 1990). In either case, low Fura-2 ratios in granules could create an artifactual region of lower $[Ca^{2+}]_i$, giving rise to gradients. To assess the behavior of Fura-2 in granules, we exploited the fact that lytic granules are connected to the endocytic pathway to load Fura-2 into granules. We incubated Tall-104 cells with Fura-2 pentapotassium salt for 2 hr at 37°C, washed them, and incubated them in Fura-free solution for 2 hr. Comparison of Fura-2 and LTR images indicates that this procedure selectively loads Fura-2 into lytic granules (Figure 5C, 1 mM Fura). We next compared in parallel experiments cellular and granule Fura-2 responses to stimulation with 1 μM TG in Ca^{2+}-free Ringer's, followed by $Ca^{2+}{}_o$ addition, and then ionomycin application (Figure 5D), a protocol that elicits robust, synchronous $[Ca^{2+}]_i$ changes in every cell. Note that 100 μM Fura-2 was used in these experiments, a concentration chosen to be similar to the concentration of Fura-2 achieved by AM-loading (Donnadieu et al., 1992). Granule Fura-2 ratios remained unchanged despite large cellular ratio changes (Figure 5D), indicating that apparent cytosolic

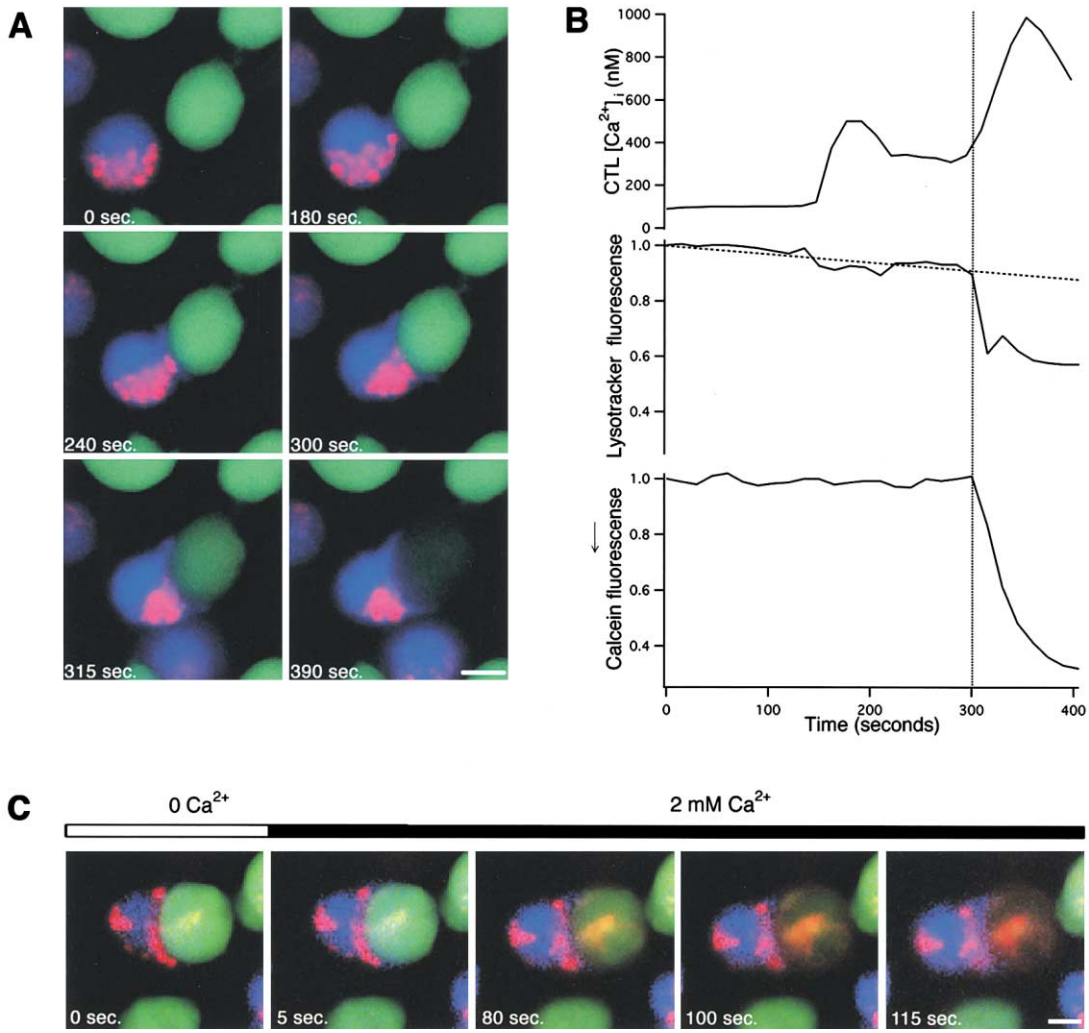

Figure 4. Detection of Target-Directed Lytic Granule Exocytosis during Killing of bsAB-Treated Raji Cells

(A) Fluorescence images of an interaction between a single TALL-104 and a bsAB-treated Raji cell. The Raji cell was loaded with calcein (green), and the TALL-104 was loaded with Fura-2 (F340 is displayed in blue.) The Ringer's solution contained 100 nM Lysotracker Red, which labeled TALL-104 lytic granules (red). Scale bar is 5.6 μm.

(B) Quantitation of TALL-104 $[Ca^{2+}]_i$ and lytic granule fluorescence and Raji cell calcein fluorescence for the experiment shown in (A).

(C) Image sequences showing killing by a Tall-104 cell that made contact with a bsAB-treated Raji cell in Ca^{2+}-free Ringer's. Ca^{2+}_o was added between the first and second frame. Scale bar is 4.6 μm.

Ca^{2+} gradients reflect contributions of low Fura-2 ratios in granules.

The results presented above suggest that $[Ca^{2+}]_i$ gradients in TALL-104 cells do not reflect the distribution of Ca^{2+} channels. Additionally, we see theoretical problems associated with the idea of sustained $[Ca^{2+}]_i$ gradients generated by polarization of influx sites in CTLs, unless substantial diffusion barriers are present within the cell. The rate of buffered Ca^{2+} diffusion in the cytosol of most cells is sufficiently rapid (10^{-7}–10^{-6} cm^2s^{-1} (Neher, 1986) and TALL-104 cells sufficiently small (diameter of ~7 μM) that $[Ca^{2+}]$ would be expected to equilibrate everywhere within a typical CTL in ~0.3–3 s, except in microdomains formed in the immediate vicinity of influx sites, where $[Ca^{2+}]$ could be persistently higher.

Store-operated Ca^{2+} channels are likely responsible for target cell stimulated Ca^{2+} influx in CTLs (Hess et al., 1993; Zweifach, 2000). As the molecular identity of these channels is unclear, and neither high-affinity blockers nor antibodies are available, we used a functional approach to assess the distribution of Ca^{2+} channels. We reasoned that if Ca^{2+} channels are polarized, we should observe a $[Ca^{2+}]$ wave emanating from the location of the channels if we suddenly triggered influx. It is necessary to trigger influx rapidly to observe waves, as target cell-stimulated $[Ca^{2+}]_i$ signals are multiphasic, reflecting the contribution of store release followed by influx and additional store release (Zweifach, 2000), so it is not possible to ascribe any part of the $[Ca^{2+}]_i$ signals specifically to influx. To determine whether waves can in fact be detected, we polarized influx artificially (Figure 6A). Cells were loaded with the single-wavelength Ca^{2+}-indicator dye fluo-3, and 1 μM thapsigargin was bath-applied in the absence of Ca^{2+}_o to activate Ca^{2+} channels

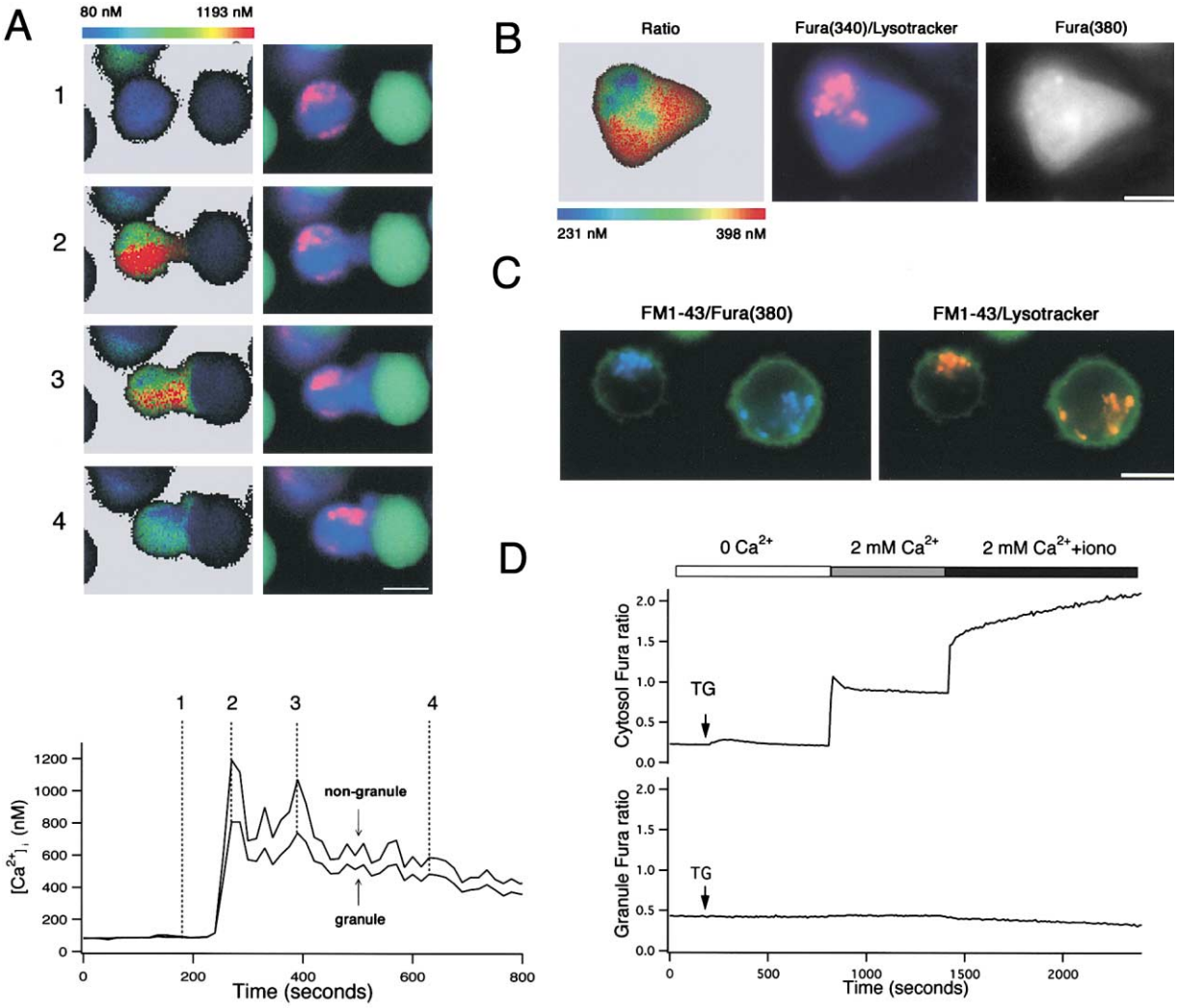

Figure 5. Sustained $[Ca^{2+}]_i$ Gradients in TALL-104 Cells Contacting Targets Are Due to Low Fura-2 Ratios in Granules

(A) Top: pseudocolored ratio and fluorescence images of a TALL-104 interacting with a bsAB-treated Raji cell. In the fluorescence image, F340 is blue, lytic granules labeled with LTR are red, and target cell calcein fluorescence is green. Scale bar is 7.5 μm. Bottom: plots of $[Ca^{2+}]$ versus time for the experiment shown above. The granule trace was computed by analyzing an ROI defined by LTR (granule) fluorescence for the mass of granules in the top half of the cell. The nongranule trace was computed analyzing the Fura-2 signal from the rest of the cell, including the small region of granules at the bottom of the cell.

(B) High-resolution images of Fura-2 ratio, F380, and lysotracker red for a TALL-104 in contact with a bsAB-treated Raji cell located at the lower right of the image. Scale bar is 4.8 μm.

(C) Extracellularly applied Fura-2 pentapotassium salt is taken up into lytic granules. FM1-43 (green) was used to label plasma membranes. Scale bar is 4.8 μm.

(D) Parallel measurement of cellular (Fura-2 AM) and granule Fura-2 ratios reveals that granule ratios remain constant as cytosolic ratios increase. Data are averages of 623 cells (Fura-2 AM) and 526 cells (Fura salt) from three experiments.

(Thastrup et al., 1989; Zweifach, 2000). We used fluo-3 because we do not have the ability to switch excitation wavelengths rapidly enough to use Fura-2 as a ratiometric dye. Gigaohm seals were formed with pipettes containing 20 mM $CaCl_2$ Ringer's. The pipette potential was clamped at −150mV to offset the diffusional driving force for Ca^{2+} to flow into the cell through channels in the patch. Imaging was initiated at 13–17 Hz, and the pipette potential was switched to +150mV to drive Ca^{2+} through channels in the patch. Analysis of images obtained from six cells with this protocol revealed that $[Ca^{2+}]_i$ rose first near the pipette, and then 513 ± 280 ms (mean ± SD) later at sites located 7.2 ± 0.4 μm away. These values correspond to a diffusion coefficient of $\sim 5 \times 10^{-7}$ $cm^2 s^{-1}$ (calculated from the relation $d = a^2/2t$, where d is the diffusion coefficient, a is the distance, and t is the delay [Neher, 1986]) within the expected range (1×10^{-7}–1×10^{-6} $cm^2 s^{-1}$ [Neher, 1986]), and indicate that imaging at rates of 13 Hz or faster is sufficient to detect $[Ca^{2+}]$ waves spreading from localized influx sites in TALL-104s. Further, that d is in the range expected for free diffusion suggests that there are no substantial diffusion barriers in TALL-104s.

To test whether channels are polarized during target

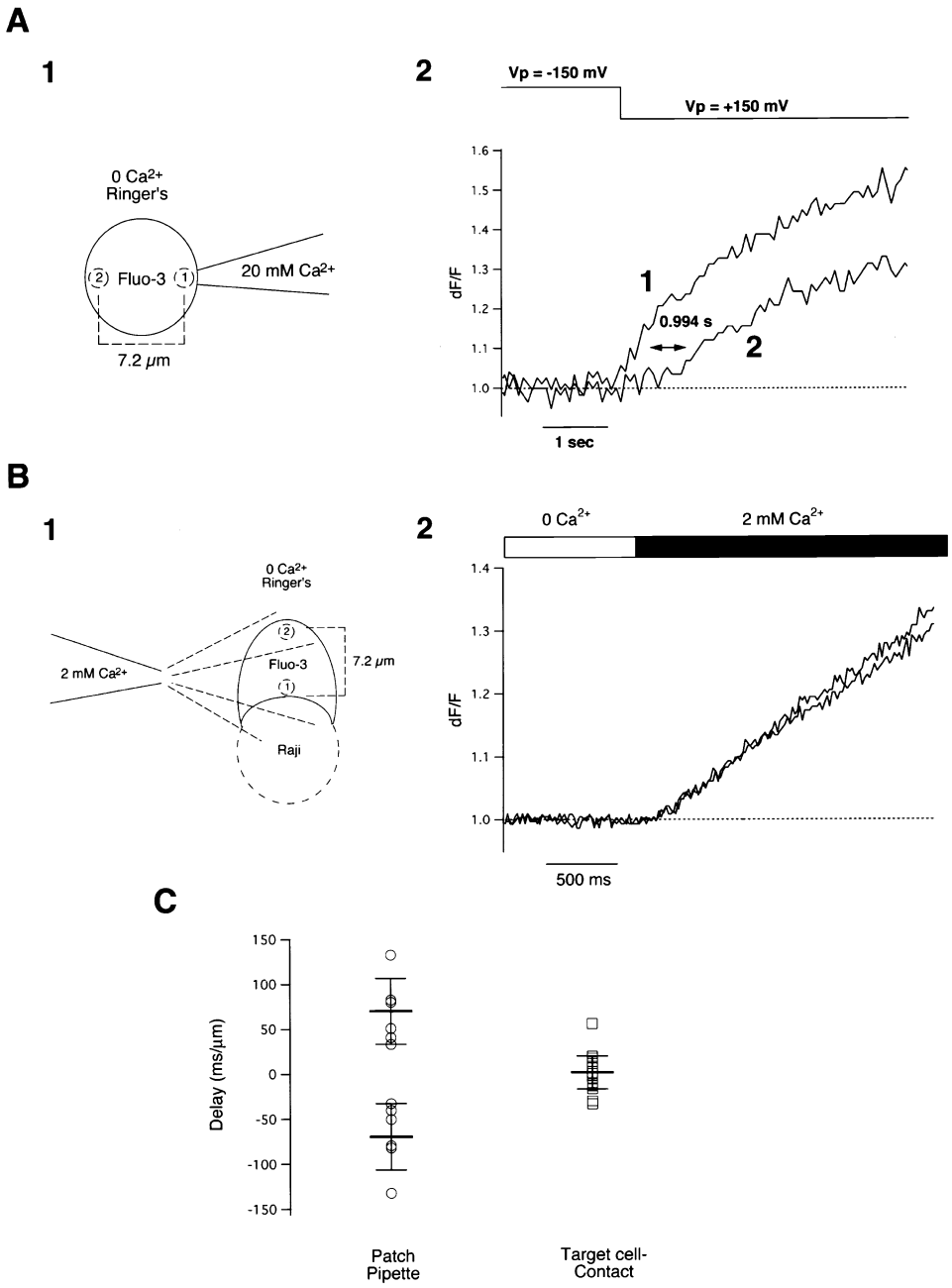

Figure 6. Rapid Imaging Experiments Indicate that Ca^{2+} Channels Are Not Polarized on TALL-104 during Target Cell Killing

(A) Detection of $[Ca^{2+}]_i$ waves when influx is polarized artificially. (1) Diagram of the experimental conditions. (2) Traces of fluo-3 fluorescence from 2 ROIs, one near the pipette and one at the cell's opposite end.

(B) Waves are not detected in TALL-104 cells contacting bsAB-treated Raji cells. (1) Diagram of the experimental conditions. (2) Traces of fluo-3 fluorescence from 2 ROIs, one near the site of contact with the target cell, the other at the opposite end of the cell.

(C) Pooled results from experiments represented in (A and B). Data from (B) are represented twice to allow comparison with data from (A). Our convention is that positive values of the distance-corrected delay correspond to channels being polarized at the site of contact with the target; negative values correspond to the opposite polarity.

cell killing (Figure 6B), we loaded TALL-104 cells with fluo-3, and allowed them to interact with bsAB-treated Raji cells in Ringer's. Cells were settled onto coverslips, and then the chamber was perfused with Ca^{2+}-free Ringer's supplemented with 1 mM EGTA. When suitable conjugates were identified, a wide-mouthed (~5 μm) puffer pipette containing Ringer's was positioned 15–20 μM away and oriented perpendicular to the front-to-back axis of the CTL to minimize inhomogeneities in the rate at which Ca^{2+}_o reached the sites of interest. Control experiments in which we examined responses of as many as four TALL-104 cells in contact with a single bsAB-treated Raji cell did not reveal delays in the delivery of Ca^{2+} from puffer pipettes. Image collection was

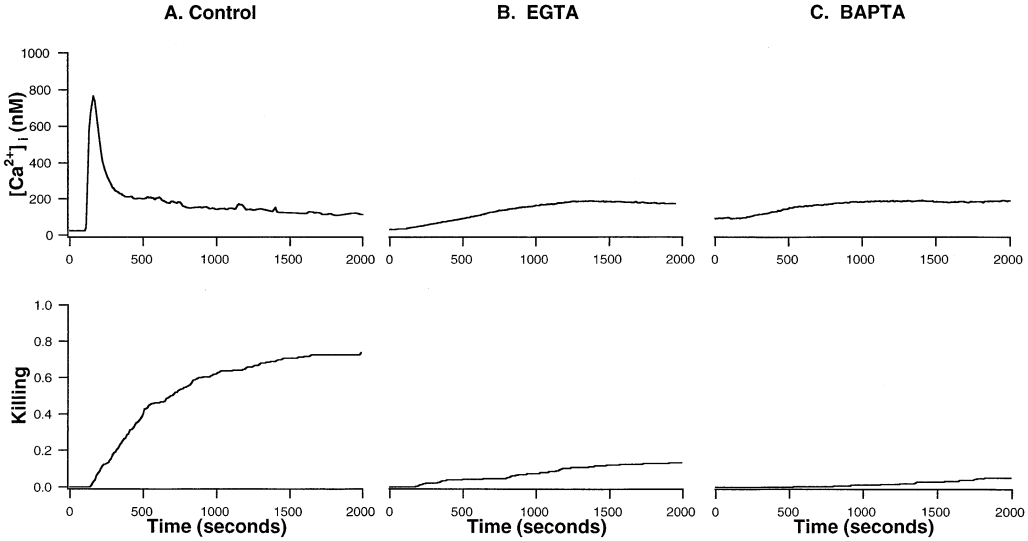

Figure 7. Suppressing $[Ca^{2+}]_i$ Increases with BAPTA or EGTA Reduces Target Cell Killing

Average $[Ca^{2+}]_i$ (top) and target cell killing (bottom) for (A) Control cells. (B) Cells loaded with EGTA-AM and (C) Cells loaded with BAPTA-AM. EGTA and BAPTA had equivalent abilities to suppress $[Ca^{2+}]_i$ increases and target cell killing. Data are the average of 419 cells (control), 348 cells (EGTA) and 288 cells (BAPTA), respectively, from triplicate experiments for the $[Ca^{2+}]_i$ traces, and 260 cells (control), 333 cells (EGTA) and 336 cells (BAPTA) from triplicate experiments for target cell killing.

started, and $Ca^{2+}{}_o$ was puffed on. For these experiments, we used a faster imaging system capable of acquiring fluo-3 images at 58 Hz. In 22 such experiments, $[Ca^{2+}]$ rose only 8.0 $\pm$ 84.7 ms earlier at the site of contact with the target than at the CTL's other edge (distance = 7.2 $\pm$ 0.4 μm), a value not significantly different than zero. These results do not support the idea that Ca^{2+} channels are polarized when TALL-104 cells contact targets.

Suppressing $[Ca^{2+}]_i$ Increases with BAPTA or EGTA Prevents Granule Exocytosis

To determine whether Ca^{2+}acts in microdomains near the membrane or at longer distances in the bulk cytosol, we compared the effects on target cell killing of loading TALL-104 cells with the Ca^{2+} chelators BAPTA and EGTA (Figure 7). These chelators have similar affinities for Ca^{2+}, but BAPTA binds Ca^{2+} ~400 $\times$ more quickly than EGTA because it does not first have to undergo deprotonation, and can thus prevent $[Ca^{2+}]$ increases within nanometers of influx sites, while EGTA cannot (Neher, 1986; Zucker, 1996). A key prerequisite in this experiment is that the two chelators suppress cytosolic $[Ca^{2+}]_i$ rises equivalently. To determine the loading conditions needed to meet this requirement, we performed experiments like the ones shown in Figure 7. We incubated TALL-104 cells with different concentrations of BAPTA-AM and EGTA-AM for 30 min at room temperature. Cells were adhered to coverslips, and bsAB-treated Raji cells were allowed to make contact for 30 min in the absence of $Ca^{2+}{}_o$. Imaging was started and the chamber was perfused with 2 mM $Ca^{2+}{}_o$ and $[Ca^{2+}]_i$ was monitored for 50 min. Loading cells with 100 μM BAPTA-AM effectively suppressed $[Ca^{2+}]_i$ increases, but it was necessary to load cells with 2.5 mM EGTA-AM to reduce $[Ca^{2+}]_i$ increases equivalently. We suspect that this difference reflects the efficacy with which the two chelators are loaded into cells. An alternative is that Ca^{2+} channels are more active in the presence of EGTA than BAPTA, and thus more EGTA is required to suppress $[Ca^{2+}]_i$ signals. Regardless, neither our results nor the conclusions we make based on them below are affected.

We next examined the effects of the two chelators on target cell killing (Figure 7). We allowed an excess of TALL-104 cells to form conjugates with bs-AB treated calcein-loaded Raji cells in Ca^{2+}-free Ringer's for 30 min. Image collection was started, and the chamber was perfused with Ringer's solution. Both BAPTA and EGTA markedly reduced the extent of target cell killing, although BAPTA was slightly more effective (Figure 7B). When granule exocytosis triggered by α-CD3 beads was monitored using BLT-esterase assays, similar effects of BAPTA and EGTA were observed (data not shown). That EGTA reduces killing provides clear evidence for an action of Ca^{2+} that does not occur in microdomains in the immediate vicinity of influx sites, and this conclusion is not dependent on the amount of EGTA required to suppress $[Ca^{2+}]_i$ signals. We conclude that Ca^{2+}has an action at sites that are located at a relatively large diffusional distance away from channels.

Discussion

We used TALL-104 leukemic cytotoxic T lymphocytes as a model system to examine the role of Ca^{2+} influx in lytic granule exocytosis. TALL-104 cells have large granules, which can easily be visualized, and when stimulated via CD3, are extremely efficient and specific killers. α-CD3-stimulated granule exocytosis and target cell killing by TALL-104 cells is characterized by key features

that have been described previously for other CTL lines: bsAB-stimulated granule exocytosis is target-directed, (Figure 4), and is absolutely dependent on Ca^{2+} influx (Figure 2). Thus, while the mechanism by which these cells recognize tumor targets remains unclear, bsAB-stimulated TCR-triggered target cell killing by TALL-104 cells is well suited to investigations of the physiology of CTL granule exocytosis.

Our method for monitoring lytic granule dynamics while simultaneously measuring CTL $[Ca^{2+}]_i$ using Fura-2 and target cell killing using calcein (Figure 4) may be useful for the study of granule dynamics and exocytosis in CTLs. Yanelli et al. used Nomarski optics to monitor the movements of lytic granules in thin mount CTL-target preparations, and reported evidence consistent with the exocytosis of lytic granules (Yanelli et al., 1986). However, Nomarski optics produce inherently thin focal planes that are very sensitive to changes of granule position in the z-axis, and do not provide a quantifiable optical signal that can be used to monitor granule release. One limitation of our method is that LTR labels structures in both CTL and target, making it difficult in some cases to measure signals quantitatively. Also, LTR is unsuitable for investigating exocytosis triggered by ionophores and PMA, as Ca^{2+}-H^+ exchange ionophores like ionomycin are likely to deacidify lytic granules (Reed and Lardy, 1972). Importantly, LTR does not affect the kinetics of target cell killing, a potential concern with a lysosomotrophic weak base, as agents that deacidify lytic granules can prevent granule exocytosis (Kataoka et al., 1994).

We detected release of ~15% of TALL-104 granules during killing of Raji cells, which is likely an upper estimate for the average release during killing, as in some cases we could see granules disappear at the site of contact with the target but could not quantitate a decrease in LTR fluorescence. We estimate that the minimum granule fluorescence decrease we could have detected was ~3% based on the noise levels of LTR fluorescence traces. That only a fraction of granules is released during killing is consistent with the observation that CTLs are capable of serial killing (we observed serial killing of bsAB-treated Raji by TALL-104 (not shown)). Decreases in LTR fluorescence occurred ~40–60 s before decreases in target cell membrane integrity suggesting that there is a delay between granule exocytosis and formation of functional perforin pores in the target cell's membrane. Previous work has shown that purified perforin assembles to form pores in membranes with a time constant of ~6 s at 37°C, and that decreasing temperature inhibits polymerization (Ishiura et al., 1990). Our experiments were conducted at room temperature and we were monitoring release of perforin from intact granules. Granule matrix componenents are known to prevent perforin from polymerizing (Tschopp and Masson, 1987; Griffiths and Argon, 1995), so the delay we measured likely includes the time needed for perforin to disassociate from other granule components, and to form functional pores in the target's membrane.

Consistent with previous reports (Poenie et al., 1987; Gray et al., 1988), we observed $[Ca^{2+}]_i$ gradients in CTLs in contact with targets (Figure 5). However, in TALL-104 cells gradients could be accounted for by the position of the lytic granules, which have been shown to contain calreticulin (Dupuis et al., 1993; Griffiths and Argon, 1995), and thus may be able to maintain low $[Ca^{2+}]$ when $[Ca^{2+}]_i$ is elevated. Alternatively, Fura-2 in granules may not be responsive to changes in $[Ca^{2+}]$ because of the granular microenvironment (Roe et al., 1990). Our results clearly indicate that granule Fura-2 ratios remain at levels indicating low $[Ca^{2+}]$ even when bulk cellular Fura-2 ratios increase (Figure 5D). Thus, the apparent cytosolic $[Ca^{2+}]_i$ gradients we observed are due to convolution of the cytosolic $[Ca^{2+}]_i$ signal with signals emanating from Fura-2 in granules. In this regard, our results are similar those of Gray et al. (Gray et al., 1988), who detected regions of low Ca^{2+}, and suggested that they corresponded to lytic granules after $[Ca^{2+}]_i$ had increased. Note that Poenie et al. provided evidence against compartmentalization of Fura-2 as the source of gradients in their experiments (Poenie et al., 1987), so the gradients they observed may not arise from the same source.

To assess the location of Ca^{2+} channels, we used rapid imaging to look for Ca^{2+} waves spreading from Ca^{2+} channels when influx was initiated rapidly (Figure 6). That we did not observe Ca^{2+} waves provides evidence that Ca^{2+} channels are not polarized on TALL-104 cells during target cell killing, and, together with the observation that bsAB-treated Raji cells elicit target-directed exocytosis (Figure 4), suggests that polarized Ca^{2+} influx is not required to direct lytic granules to the contact site. Compartmentalization of dye in granules is unlikely to affect our results, as areas of cells that contain granules still give $[Ca^{2+}]_i$ responses, although the amplitude of the responses is reduced (Figure 5). For this reason, redistribution of granules due to perturbation by the patch pipette in experiments in which influx was polarized artificially is unlikely to affect our results, even if it occurred. One possible caveat to the conclusion that channels are not clustered on CTLs is that to detect waves we had to incubate cells in Ca^{2+}-free extracellular solution following conjugate formation in Ca^{2+}-containing Ringer's. We did this to decrease $[Ca^{2+}]_i$, so that $Ca^{2+}{}_o$ readdition would cause a rapid $[Ca^{2+}]_i$ increase that we could detect as a wave. It is possible that elevated $[Ca^{2+}]_i$ is required for the maintenance of channel clustering, although if this is the case a signal would be required to direct Ca^{2+} channel reclustering following $Ca^{2+}{}_o$ readdition, and thus Ca^{2+} channels themselves could not be the primary signal governing cell polarity. If granules are not directed by $[Ca^{2+}]$ gradients, how might they be directed? Recent work has shown that a number of T cell signaling molecules, including PLC-γ, PI-3K, Itk, PKC-θ and Ras cluster at the site of contact with targets/APCs (Bromley et al., 2001). One of these molecules may provide directional cues for granule reorientation.

That EGTA suppresses target cell killing (Figure 7) provides evidence for an action of Ca^{2+} that occurs at a relatively large diffusional distance from Ca^{2+} channels rather than in microdomains. Bulk $[Ca^{2+}]_i$ measurements obtained with Fura-2 can be used to estimate the $[Ca^{2+}]$ relevant for this action. $[Ca^{2+}]_i$ increased to levels ranging from 0.3–2 μM following target cell contact in Ringer's solution containing 2 mM $Ca^{2+}{}_o$ (Figures 1, 4, 5, and 7), suggesting that the affinity for Ca^{2+} is less than 2 μM. $Ca^{2+}{}_o$ can be reduced to 100 μM without affecting the extent or rate of either target cell killing or granzyme

release (our unpublished observations). Under these conditions, $[Ca^+]_i$ increases to maximal levels of only ~500 nM, suggesting that $[Ca^{2+}]$ less than 1 μM are sufficient to support maximal granule exocytosis. Our $[Ca^{2+}]_i$ measurements are unlikely to be affected significantly by compartmentalization of Fura-2 in granules, as excluding granules from analysis increases measured $[Ca^{2+}]_i$ by only 50–100 nM (Figure 5B). CTLs thus behave similarly to mast cells, in which $[Ca^{2+}] < 1$ μM are sufficient to support maximal exocytosis in permeabilized cells (Hide et al., 1993). Also similar to mast cells is the slow time course of exocytosis following an increase in $[Ca^{2+}]$, which is consistent with a dependence of granule exocytosis on global $[Ca^{2+}]_i$. One striking difference between mast cell exocytosis and lytic granule exocytosis, however, is that mast cells release most of their granules upon stimulation (Hide et al., 1993); CTLs appear to release only a subset of their granules during target cell killing.

Conventional lysosomes are exocytosed in response to $[Ca^{2+}]_i$ increases of 1–5 μM (Rodriguez et al., 1997). Exocytosis of CTL secretory lysosomes and conventional lysosomes therefore shares a similar high-affinity requirement for Ca^{2+}. As synaptotagmin VII is a candidate high-affinity Ca^{2+} binding protein in exocytosis of conventional lysosomes (Martinez et al., 2000), it may play this role in the exocytosis of CTL lytic granules. However, unlike conventional lysosomes, granule exocytosis cannot be triggered simply by agents that increase $[Ca^{2+}]_i$, but also requires activation of PKC (Berebi et al., 1987; Lancki et al., 1987). Another candidate for a high-affinity Ca^{2+} binding protein in CTL granule exocytosis is the Ca^{2+}-dependent phosphatase calcineurin, which underlies the Ca^{2+}-dependence of helper T cell activation (Crabtree, 1989). Calcineurin inhibitors such as FK506 and cyclosporin A block CTL granule exocytosis (Dutz et al., 1993), and we find that these agents inhibit granule exocytosis in TALL-104 cells (our unpublished observations).

Finally, as CTL granule exocytosis is a complex process involving cytoskeletal reorganization and granule reorientation in addition to fusion of granules with the plasma membrane, there may be multiple Ca^{2+}-dependent steps involved. The delay between initial $[Ca^{2+}]_i$ increases and granule exocytosis is long enough to encompass multiple Ca^{2+}-dependent steps. Our data suggest that Ca^{2+} is required for an early and/or rate-limiting step in granule exocytosis, as contact between CTLs and targets in $Ca^{2+}{}_o$-free solution did not accelerate the rate of target cell killing after $Ca^{2+}{}_o$ was added, compared to experiments in which contact was made in the presence of $Ca^{2+}{}_o$ (Figure 2C). Previous work has shown that reorientation of the CTL's MTOC to the site of contact with the target requires $Ca^{2+}{}_o$ (Kupfer et al., 1983; Kupfer and Dennert, 1984), and thus presumably requires $[Ca^{2+}]_i$ increases. Our results suggest that the early step we have identified is not reorientation of lytic granules, since cells that made contact with their granules oriented toward target cells, did not kill faster than cells that made contact with their granules in other orientations. Of course, if $[Ca^{2+}]_i$ increases are required for an early or rate-limiting step in granule exocytosis, then it is possible that other later steps also require $[Ca^{2+}]_i$ elevation.

Experimental Procedures

Chemicals and Reagents

Salts for physiological solutions, N-(-benzyloxycarbonyl-L-lysine thiobenzyl ester (BLT), 5,5′-dithio-bis-(2-nitrobenzioic acid) (DTNB), and poly-L-lysine were from Sigma-Aldrich (St. Louis, Missouri). Fura-2 AM, calcein AM, FM1-43, and lysotracker red (LTR) were from Molecular Probes (Eugene, Oregon). Thapsigargin and the FITC-conjugated anti-perforin mAB were purchased from Alexis Biochemicals (San Diego, California). Fetal calf serum, glutamine, and antibiotics were purchased from Gemini Bioproducts (Calabassas, California). Recombinant human IL-2 was obtained from Chiron, Inc. (Emeryville, California). α-CD3 beads (M-450 Pan T) were purchased from Dynal A.S. (Oslo, Norway). The bispecific antibody (bsAB; Hu1D10-Jun × HuM291-Fos) was a gift from Protein Design Laboratories, Inc. (Mountain View, California.)

Cells

Raji B lymphoma cells were grown in RPMI supplemented with 10% FCS. TALL-104 cells were grown in Iscove's medium supplemented with 20% FCS and 100 IU IL-2. Both cell types were grown in a humidifed incubator at 37°C in 10% CO_2. Raji cells were loaded with calcein by incubating them with 1 μM calcein-AM in cell culture medium for 30 min. at room temperature, and were treated with bsAB by incubating them in the presence of 320 μg/ml bsAB in Ringer's solution for 15 min at room temperature. TALL 104 cells were loaded with Fura-2 by incubating them with 1 μM Fura-2 AM in cell culture medium for 30 min. at room temperature. Cells were washed twice with fresh medium before use.

Solutions

Ringer's solution contained (in mM): 145 NaCl, 4.5 KCl, 1 $MgCl_2$, 2 $CaCl_2$, 5 HEPES and 10 glucose (pH 7.4 with NaOH). Zero Ca^{2+} Ringer's was identical, except $CaCl_2$ was replaced with $MgCl_2$. Zero Ca^{2+} Ringer's plus EGTA was identical to zero Ca^{2+} Ringer's, but was supplemented with 1 mM EGTA.

Imaging

Most experiments were performed with an imaging system described previously (Zweifach, 2000). Fura-2 ratio data were analyzed as described previously (Zweifach, 2000). To analyze CTL granule fluorescence signals, we first segmented images on F340. As calcein, used to follow Raji membrane integrity, is also fluorescent in the wavelengths used to excite Fura-2, this procedure selected a region of interest (ROI) that corresponded to both the TALL-104 and the target cell. We then segmented images on FITC, and performed an exclusive "OR" operation, yielding an ROI that corresponded with reasonable fidelity to the fluorescence of the TALL-104 alone, allowing discrimination of CTL-associated lyostracker red fluorescence. In some cases, the ROI selected automatically was modified by hand to conform better to the outline of the cell.

For experiments in which influx was polarized artificially, patch clamp techniques were performed as described previously (Zweifach and Lewis, 1993). Rapid imaging experiments to determine the location of channels on CTLs in contact with targets were performed on a Till Photonics imaging system built around a Nikon Diaphot microscope using a Till Imago VGA CCD and a Till monochromater. A Nikon 100 × fluor objective (NA = 1.4) was used, and the CCD chip was binned 4 × 4. Under these conditions, a maximum image acquisition rate of 58 Hz could be maintained for ~3 s. Delays between $[Ca^{2+}]_i$ increases at different regions of cells were determined by shifting traces in time until they were best aligned as determined by eye. This procedure yielded comparable results to analysis strategies using arbitrary thresholds.

BLT-Esterase Assays

BLT-esterase activity released from TALL-104 cells essentially as described previously (Takayama et al., 1987).

Immunocytochemistry

TALL-104 cells were adhered to poly-L-lysine coated coverslips in medium, then washed with PBS containing 100 nM LTR and incubated for 10 min at room temperature. Cells were fixed with 3.7%

formaldehyde in PBS supplemented with 120 mM sucrose, and then permeabilized by incubation with chilled 100% methanol at −15°C for 15 min. After thorough washing with PBS, samples were blocked by incubation in PBS + 15% goat serum for 1 hr. Samples were then incubated with PBS + 15% goat serum + 2.5 μg/ml FITC-labeled anti-perforin mAB at room temperature overnight, and then washed extensively with PBS. Images were acquired using the imaging system described above.

Statistics

Except where noted, all results are presented as mean ± S.E.M.

Acknowledgments

We thank Dr. S. R. Levinson for help with immunocytochemistry, and Dr. William J. Betz for the use of the Till Photonics imaging system. We also thank Dr. Yiannis Koutalos and Dr. Robert Zorec for helpful discussions. Supported by NIH grant AI42964

Received April 5, 2001; revised September 26, 2001.

References

Berebi, G., Takayama, H., and Sitkovsky, M.V. (1987). Antigen-receptor interaction requirement for conjugate formation and lethal-hit triggering by cytotoxic T lymphocytes can be bypassed by protein kinase C activators and calcium ionophores. Proc. Natl. Acad. Sci. USA *84*, 1364–1368.

Berke, G. (1994). The binding and lysis of target cells by cytotoxic lymphocytes: molecular and cellular aspects. Annu. Rev. Immunol. *12*, 736–753.

Betz, W.J., Mao, F., and Smith, C.B. (1996). Imaging exocytosis and endocytosis. Curr. Opin. Neurobiol. *6*, 365–371.

Bromley, S.K., Burack, W.R., Johnson, K.G., Somerslao, K., Sims, T.N., Sumen, C., Davis, M.M., Shaw, A.S., Allen, P.M., and Dustin, M.L. (2001). The immunological synapse. Annu. Rev. Immunol. *19*, 375–396.

Burkhardt, J.K., Hester, S., Lapham, C.K., and Argon, Y. (1990). The lytic granules of natural killer cells are dual-function organelles combining secretory and pre-lysosomal compartments. J. Cell. Biol. *111*, 2327–2340.

Cesano, A., and Santoli, D. (1992). Two unique human leukemic T-cell lines endowed with a stable cytotoxic function and a different spectrum of target reactivity analysis and modulation of their lytic mechanisms. In Vitro Cell. Dev. Biol. *28A*, 648–656.

Crabtree, G.R. (1989). Contingent genetic regulatory events in T lymphocyte activation. Science *243*, 355–361.

Donnadieu, E., Bismuth, G., and Trautmann, A. (1992). Calcium fluxes in T lymphocytes. J. Biol. Chem. *267*, 25864–25872.

Dupuis, M., Schaerer, E., Krause, K., and Tschopp, J. (1993). The calcium-binding protein calreticulin is a major constituent of lytic granules in cytolytic T lymphocytes. J. Exp. Med. *177*, 1–7.

Dutz, J.P., Fruman, D.A., Burakoff, S.J., and Bierer, B.E. (1993). A role for calcineurin in degranulation of murine cytotoxic T lymphocytes. J. Immunol. *150*, 2591–2598.

Gray, L.S., Gnarra, J.R., Sullivan, J.A., Mandell, G.L., and Engelhard, V.H. (1988). Spatial and temporal characterstics of the increase in intracellular calcium induced in cytotoxic T lymphocytes by cellular antigen. J. Immunol. *141*, 2424–2430.

Griffiths, G.M. (1995). The cell biology of CTL killing. Curr. Opin. Immunol. *7*, 343–348.

Griffiths, G.M., and Argon, Y. (1995). Structure and biogenesis of lytic granules. Curr. Top. Microbiol. Immunol. *198*, 39–58.

Haller, T., Ortmayr, J., Friedrich, F., Volkl, H., and Dietl, P. (1998). Dynamics of surfactant release in alveolar type II cells. Proc. Natl. Acad. Sci. USA *95*, 1579–1584.

Hess, S.D., Oortgiesen, M., and Cahalan, M.D. (1993). Calcium oscillations in human T and natural killer cells depend upon membrane potential and calcium influx. J. Immunol. *150*, 2620–2633.

Hide, I., Bennet, J., Pizzey, A., Booney, G., Bar-Sagi, D., Gomperts, B., and Tatham, P. (1993). Degranulation of individual mast cells in response to Ca^{2+} and guanine nucleotides: an all-or-none event. J. Cell. Biol. *123*, 585–593.

Ishiura, S., Matsuda, K., Koizumi, H., Tsukahara, T., Arahata, K., and Sugita, H. (1990). Calcium is essential for both the membrane binding and lytic activity of pore-forming protein (perforin) from cytotoxic T-lymphocyte. Mol. Immunol. *27*, 803–807.

Kataoka, T., Takaku, K., Magae, J., Shinohara, N., Takayama, H., Kondo, S., and Nagai, K. (1994). Acidification is essential for maintaining the structure and function of lytic granules of CTL. Effect of concanamycin A, an inhibitor of vacuolar type H^+-ATPase, on CTL-mediated cytotoxicity. J. Immunol. *153*, 3938–3947.

Kim, T., Eddlestone, G., Mahmoud, S., Kuchtey, J., and Fewtrell, C. (1997). Correlating Ca^{2+} responses and secretion in individual RBL-2H3 mucosal mast cells. J. Biol. Chem. *272*, 31225–31229.

Kupfer, A., and Singer, S.J. (1989). Cell biology of cytotoxic and helper T cell functions. Annu. Rev. Immunol. *7*, 309–337.

Kupfer, A., and Dennert, G. (1984). Reorientation of the microtubule-organizing center and the Golgi apparatus in cloned cytotoxic lymphocytes triggered by binding to lysable target cells. J. Immunol. *133*, 2762–2766.

Kupfer, A., Dennert, G., and Singer, S.J. (1983). Polarizaton of the Golgi apparatus and the microtubule-organizing center within cloned natural killer cells bound to their targets. Proc. Natl. Acad. Sci. USA *80*, 7224–7228.

Lancki, D.W., Weiss, A., and Fitch, F.W. (1987). Requirements for triggering of lysis by cytolytic T lymphocyte clones. J. Immunol. *138*, 3646–3653.

Lichtenfels, R., Biddison, W.E., Schulz, H., Vogt, A.B., and Martin, R. (1994). CARE-LASS (calcein-release-assay), an improved fluorescence-based test system to measure cytotoxic T lymphocyte activity. J. Immunol. Methods. *172*, 227–239.

Link, B., Kostelny, S., Cole, MS, Fusselman, W., Tso, J., and Weiner, G. (1998). Anti-CD3-based bispecific antibody designed for therapy of human B-cell malignancy can induce T-cell activation by antigen-dependent and antigen independent mechanisms. Int. J. Cancer *77*, 251–256.

Martinez, I., Chakrabarti, S., Hellevik, T., Morehead, J., Fowler, K., and Andrews, N. (2000). Synaptotagmin VII regulates Ca^{2+}-dependent exocytosis of lysosomes in fibroblasts. J. Cell. Biol. *148*, 1141–1149.

Neher, E. (1986). Concentration profiles of intracellular calcium in the presence of a diffusible chelator. Exp. Brain. Res. *14*, 80–96.

Poenie, M., Tsien, R.Y., and Schmitt-Verhulst, A.-M. (1987). Sequential activation and lethal hit measured by $[Ca^{2+}]_i$ in individual cytolytic T cells and targets. EMBO J. *6*, 2223–2232.

Reed, P., and Lardy, H. (1972). A23187: a divalent cation ionophore. J. Biol. Chem. *247*, 6970–6977.

Rodriguez, A., Webster, P., Ortego, J., and Andrews, N.A. (1997). Lysosomes behave as Ca^{2+}-regulated exocytic vesicles in fibroblasts and epithelial cells. J. Cell. Biol. *137*, 93–104.

Roe, M., Lemasters, J., and Herman, B. (1990). Assessment of Fura-2 for measurements of cytosolic free calcium. Cell Calcium *11*, 63–73.

Stinchcombe, J., and Griffiths, G. (1999). Regulated Secretion from hematopoietic cells. J. Cell Biol. *147*, 1–5.

Takayama, H., and Sitkovsky, M. (1987). Antigen receptor-regulated exocytosis in cytotoxic T lymphocytes. J. Exp. Med. *166*, 725–743.

Takayama, H., Trenn, G., and Sitkovsky, M.V. (1987). A novel cytotoxic T lymphocyte activation assay: optimized conditions for antigen receptor triggered granule enzyme secretion. J. Immunol. Meth. *104*, 183–190.

Thastrup, O., Dawson, A.P., Scharff, O., Foder, B., Cullen, P.J., Drobak, B.K., Bjerrum, P.J., Christensen, S.B., and Hanley, M.R. (1989). Thapsigargin, a novel molecular probe for studying intracellular calcium release and storage. Agents Actions *27*, 17–23.

Tschopp, J., and Masson, D. (1987). Inhibition of the lytic activity of perforin (cytolysin) and of late complement components by proteoglycans. Mol. Immunol. *24*, 907–913.

Yanelli, J.R., Sullivan, J.A., Mandell, G.L., and Engelhard, V.H. (1986).

Reorientation and fusion of cytotoxic T lymphocyte granules after interaction with target cells as determined by high resolution cinemicrography. J. Immunol. *136*, 377–382.

Zucker, R.S. (1996). Exocytosis: A molecular and physiological perspective. Neuron *17*, 1049–1055.

Zweifach, A. (2000). Target cell contact activates a highly selective capacitative calcium entry pathway in cytotoxic T lymphocytes. J. Cell Biol. *148*, 603–614.

Zweifach, A., and Lewis, R.S. (1993). Mitogen-regulated Ca^{2+} current of T lymphocytes is activated by depletion of intracellular Ca^{2+} stores. Proc. Natl. Acad. Sci. USA *90*, 6295–6299.